Adipose tissue is a critical regulator of osteoarthritis

Kelsey H. Collins[a,b,c], Kristin L. Lenz[a,b,c], Eleanor N. Pollitt[a,b,c], Daniel Ferguson[d], Irina Hutson[d], Luke E. Springer[e], Arin K. Oestreich[a,b,c], Ruhang Tang[a,b,c], Yun-Rak Choi[f], Gretchen A. Meyer[a,g], Steven L. Teitelbaum[h], Christine T. N. Pham[e], Charles A. Harris[d,1], and Farshid Guilak[a,b,c,2]

[a]Department of Orthopaedic Surgery, Washington University, St. Louis, MO 63110; [b]Shriners Hospitals for Children, St. Louis, MO 63110; [c]Center of Regenerative Medicine, Washington University, St. Louis, MO 63110; [d]Division of Endocrinology, Washington University, St. Louis, MO 63110; [e]Division of Rheumatology, Washington University, St. Louis, MO 63110; [f]Yonsei University College of Medicine, Seoul 120-752, South Korea; [g]Program in Physical Therapy, Washington University, St. Louis, MO 63110; and [h]Department of Pathology and Immunology, Washington University, St. Louis, MO 63110

Edited by Kristi S. Anseth, University of Colorado, Boulder, CO, and approved November 24, 2020 (received for review October 8, 2020)

Osteoarthritis (OA), the leading cause of pain and disability worldwide, disproportionally affects individuals with obesity. The mechanisms by which obesity leads to the onset and progression of OA are unclear due to the complex interactions among the metabolic, biomechanical, and inflammatory factors that accompany increased adiposity. We used a murine preclinical model of lipodystrophy (LD) to examine the direct contribution of adipose tissue to OA. Knee joints of LD mice were protected from spontaneous or posttraumatic OA, on either a chow or high-fat diet, despite similar body weight and the presence of systemic inflammation. These findings indicate that adipose tissue itself plays a critical role in the pathophysiology of OA. Susceptibility to posttraumatic OA was reintroduced into LD mice using implantation of a small adipose tissue depot derived from wild-type animals or mouse embryonic fibroblasts that undergo spontaneous adipogenesis, implicating paracrine signaling from fat, rather than body weight, as a mediator of joint degeneration.

leptin | adipocyte | subchondral bone sclerosis | muscle weakness | systemic inflammation

Osteoarthritis (OA) is the leading cause of pain and disability worldwide and is associated with increased all-cause mortality and cardiovascular disease (1, 2). OA is strongly associated with obesity, suggesting that either increased biomechanical joint loading or systemic inflammation and metabolic dysfunction related to obesity are responsible for joint degeneration (1, 2). However, increasing evidence is mounting that changes in biomechanical loading due to increased body mass do not account for the severity of obesity-induced knee OA (1–9). These observations suggest that other factors related to the presence of adipose tissue and adipose tissue-derived cytokines—termed adipokines—play critical roles in this process and other musculoskeletal conditions (1, 2, 6, 7, 10). As there are presently no disease-modifying OA drugs available, direct evidence linking adipose tissue and cartilage health could provide important mechanistic insight into the natural history of OA and obesity and therefore guide the development and translation of novel OA therapeutic strategies designed to preserve joint health.

The exact contribution of the adipokine-signaling network in OA has been difficult to determine due to the complex interactions among metabolic, biomechanical, and inflammatory factors related to obesity (11). To date, the link between increased adipose tissue mass and OA pathogenesis has largely been correlative (6, 7, 12), and, as such, the direct effect of adipose tissue and the adipokines it releases has been difficult to separate from other factors such as dietary composition or excess body mass in the context of obesity, which is most commonly caused by excessive nutrition (2, 6, 7). In particular, leptin, a proinflammatory adipokine and satiety hormone secreted proportionally to adipose tissue mass is most consistently increased in obesity-induced OA (1), and leptin knockout mice are protected from OA (6, 7). However, it remains to be determined whether leptin directly contributes to OA pathogenesis, independent of its effect on metabolism (and weight). Additional adipokines that have been implicated in the onset and progression of OA include adiponectin, resistin, visfatin, chimerin, and inflammatory cytokines such as interleukin-1 (IL-1), IL-6, and tumor necrosis factor-α (TNF-α) (13). The infrapatellar fat pad represents a local source of adipokines within the knee joint, but several studies indicate strong correlations with visceral adipose tissue, outside of the joint organ system, with OA severity (14). Furthermore, adipokine receptors are found on almost all cells within the joint and, therefore, could directly contribute to OA pathogenesis through synovitis, cartilage damage, and bone remodeling (13). The role of other adipokines (15) in OA pathogenesis remains to be determined, as it has been difficult to separate and directly test the role of adipokines from other biomechanical, inflammatory, and metabolic factors that contribute to OA pathogenesis.

To directly investigate the mechanisms by which adipose tissue affects OA, we used a transgenic mouse with lipodystrophy (LD) that completely lacks adipose tissue and, therefore, adipokine signaling. The LD model system affords the unique opportunity to directly examine the effects of adipose tissue and its secretory factors on musculoskeletal pathology without the confounding effect of diet (16, 17). While LD mice completely lack adipose tissue depots, they demonstrate similar body mass to wild-type (WT) controls on a chow diet (12, 16–19). These characteristics provide a unique model that can be used to eliminate the factor of loading due to body mass on joint damage and, thus, to directly

Significance

Obesity is a primary risk factor for osteoarthritis, involving complex interactions among the metabolic, biomechanical, and inflammatory factors caused by increased adiposity. Using a mouse model of lipodystrophy, we demonstrate that fat-free mice on either a chow or high-fat diet are protected from cartilage damage, despite demonstrating many factors previously associated with osteoarthritis. Furthermore, implantation of a small fat pad reverses cartilage protection in lipodystrophic mice, indicating a direct relationship between adipose tissue and cartilage damage, independent of body weight. This study provides evidence of adipose–cartilage signaling, indicating that tissues outside the joint can influence cartilage health. These findings support the notion that osteoarthritis involves a systemic component, providing insight into the development of new therapeutic targets for osteoarthritis.

Author contributions: K.H.C., D.F., A.K.O., G.A.M., S.L.T., C.T.N.P., C.A.H., and F.G. designed research; K.H.C., K.L.L., E.N.P., I.H., L.E.S., R.T., and Y.-R.C. performed research; C.A.H. contributed new reagents/analytic tools; K.H.C., K.L.L., E.N.P., I.H., L.E.S., and R.T. analyzed data; and K.H.C., C.T.N.P., and F.G. wrote the paper.

The authors declare no competing interest.

This article is a PNAS Direct Submission.

[1]Present address: Early Clinical Development & Experimental Sciences, Regeneron Pharmaceuticals, Tarrytown, NY 10591.

[2]To whom correspondence may be addressed. Email: guilak@wustl.edu.

This article contains supporting information online at https://www.pnas.org/lookup/suppl/doi:10.1073/pnas.2021096118/-/DCSupplemental.

Published December 21, 2020.

test the effects of fat and factors secreted by fat on musculoskeletal tissues. Of particular interest, LD mice also exhibit several characteristics that have been associated with OA, including sclerotic bone (11, 20), metabolic derangement (3, 5, 7–9, 21, 22), and muscle weakness (2). Despite these OA-predisposing features, LD mice are protected from OA and implantation of adipose tissue back into LD mice restores susceptibility to OA—demonstrating a direct relationship between adipose tissue and cartilage health, independent of the effect of obesity on mechanical joint loading.

Results

Male and Female LD Mice Demonstrate Metabolic Dysfunction and Systemic Inflammation. On a chow control diet, both male and female LD mice demonstrated similar total body mass (Fig. 1*A*) compared to their same-sex WT littermate controls. Body fat, measured by both dual-energy X-ray absorptiometry (DXA) and quantitative magnetic resonance technology (EchoMRI), was significantly reduced in LD mice (Fig. 1*B*), while lean mass (Fig. 1*C*) was similar, but liver mass was significantly increased in both male and female LD mice (Fig. 1*D*) compared to WT mice. LD mice lacked fat pads throughout the body, including the infrapatellar fat pad normally found in the knee of WT mice (*SI Appendix*, Fig. S1).

To assess metabolic dysfunction, insulin-tolerance tests and glucose-tolerance tests were performed. Insulin-tolerance tests revealed overt insulin resistance in LD animals compared to WT littermates, as evidenced by a significant increase in blood glucose levels from baseline (Fig. 1*E*). A main effect of genotype and interaction of genotype by sex was significant in glucose-tolerance tests, but the area under the curve (AUC) was not different between groups (Fig. 1*F*).

Systemic inflammatory profiles of male and female LD mice indicated similar increases in the proinflammatory mediators IL-1α, IL-1β, IL-6, TNF-α, macrophage chemoattractant protein-1 (MCP-1), and macrophage inflammatory protein-1α (MIP-1α) (Fig. 1 *G*–*L*) compared to WT levels. However, LD mice also demonstrated increased levels of the antiinflammatory mediators IL-10, tissue inhibitor of metalloproteinases-1 (TIMP-1), and IL-4 when compared to WT mice (Fig. 1 *M*–*O*). Negligible levels of leptin were detected in serum from male and female LD mice (Fig. 1*P*).

Chow-Fed LD Mice Demonstrate Reduced Activity and Muscle Weakness. To phenotype the activity and metabolic characteristics of the LD mice, we used indirect calorimetry over the period of 36 h (two dark cycles). No sex differences were observed within each genotype in any of the outcomes assessed. LD mice had reduced oxygen consumption and energy expenditure (Fig. 2 *A* and *B*). Consistent with a shift toward fat metabolism, LD mice demonstrated a decreased respiratory exchange ratio (Fig. 2*C*) and reduced CO_2 production when compared with WT control animals (Fig. 2*D*). LD and WT mice consumed similar amounts of food and water (Fig. 2 *E* and *F*) and exhibited similar energy balance (Fig. 2*G*). LD mice, however, demonstrated decreased locomotor activity (Fig. 2*H*) and ambulatory activity (Fig. 2*I*) compared to WT mice over the observation period. Consistent with this reduced activity, LD mice exhibited significantly lower forelimb grip strength when assessed at 16 and 28 wk of age (Fig. 2*J*). There was a significant effect of sex and genotype, such that female mice of both genotypes were weaker than their male counterparts. For systemic inflammatory profiles of these animals, see *SI Appendix*, Table S1.

LD Mice Are Protected from Cartilage Damage and Pain-Related Behaviors. Since LD mice show many characteristics that have been implicated in the pathogenesis of knee OA, including subchondral bone sclerosis, metabolic disturbance, inflammation, muscle weakness, and decreased activity levels, we measured the severity of OA in LD knee joints at 28 wk of age. Unexpectedly, LD mice exhibited significantly reduced spontaneous knee joint damage in both male and female animals, as measured by Modified Mankin Scores (Fig. 3 *A* and *D*). Next, we challenged the LD animals with a traumatic knee injury using destabilization of the medial meniscus (DMM) surgery. In WT mice, both males and females demonstrated significantly increased damage in DMM joints compared to their nonsurgical contralateral limbs, although female WT mice showed less severe OA as compared to male WT counterparts. In contrast, both male and female LD mice were protected from DMM-induced knee joint damage (Fig. 3 *B* and *E*). We observed increased synovitis as defined by histology scoring in DMM knee joints of LD mice compared to contralateral nonsurgical knees as well as surgical and nonsurgical knee joints of WT mice (Fig. 3 *C* and *F*). There was a trend toward increased osteophytes in DMM limbs of both groups, but the main effect of surgery was not significant ($P = 0.07$) (Fig. 3 *B* and *G*).

As sclerotic subchondral bone is widely implicated in OA onset and pathogenesis, we assessed bone microstructure of LD mice and compared it to WT mice using micro-computed tomography (microCT) analysis. LD genotype, but not sex or surgery, drove significant increases in male and female bone mineral density (BMD) in the medial tibial plateau (Fig. 3 *H* and *I*). In addition to genotype, a significant main effect of surgical intervention was observed in medial tibial plateau bone volume/total volume (BV/TV), and a significant interaction between sex and genotype was seen. Tibial metaphysis BMD also demonstrated significant main effects of sex and genotype. Tibial metaphysis BV/TV exhibited a significant main effect of sex and genotype, and significant interactions between sex × limb and sex × genotype were observed. Trabecular thickness, trabecular number, BMD, and BV/TV for the lateral tibial plateau, medial femoral condyle, and the medial tibial plateau generally showed significant effects of genotype. Detailed site-specific outcomes for each bone microstructure parameter were also described and compared (*SI Appendix*, Table S2). Generally, LD mice demonstrate a strong increased bone mass phenotype when compared to WT littermate controls.

We performed tests to quantify pain-related behaviors (i.e., knee hyperalgesia and tactile allodynia) to evaluate if LD mice develop increased pain sensitivity as a consequence of DMM despite an absence of cartilage damage. LD mice exhibited significantly higher paw-withdrawal thresholds when the DMM paw was subjected to an Electronic Von Frey assay to determine tactile allodynia (Fig. 3*J*) compared to WT animals. Furthermore, LD mice maintained similar pressure-pain thresholds in both the surgical and nonsurgical contralateral knee, while WT DMM knee joints demonstrated knee hyperalgesia.

High-Fat Diet Does Not Exacerbate the Proinflammatory Profile of LD Mice. A high-fat diet (HFD) has been shown to increase adiposity and low-grade systemic inflammation that are associated with cartilage degeneration and OA (1, 2). Given the inability of LD mice to store fat, we next sought to determine if a HFD would worsen the metabolic disturbance and inflammatory profiles observed in LD mice and, therefore, override the protection we observed in LD cartilage. Beginning at weaning, LD and WT male and female animals were fed either a 60% kilocalorie (kcal) from fat diet or 10% kcal from fat chow diet. In WT mice, body mass and body fat were increased with HFD. However, LD mice fed HFD had no change in body mass or body fat and were similar to LD and WT mice on a chow diet (Fig. 4 *A* and *B*). Lean mass at 28 wk was significantly reduced in both the LD and WT HFD-fed animals (Fig. 4*C*) as compared to both genotypes on the chow diet. Liver mass was elevated in LD mice compared to WT mice but not significantly increased between chow and HFD (Fig. 4*D*).

In LD mice, a HFD did not worsen insulin tolerance in either genotype, such that HFD LD and WT mice were similar to their chow-fed WT counterparts (Fig. 4 *E* and *F*). Glucose tolerance,

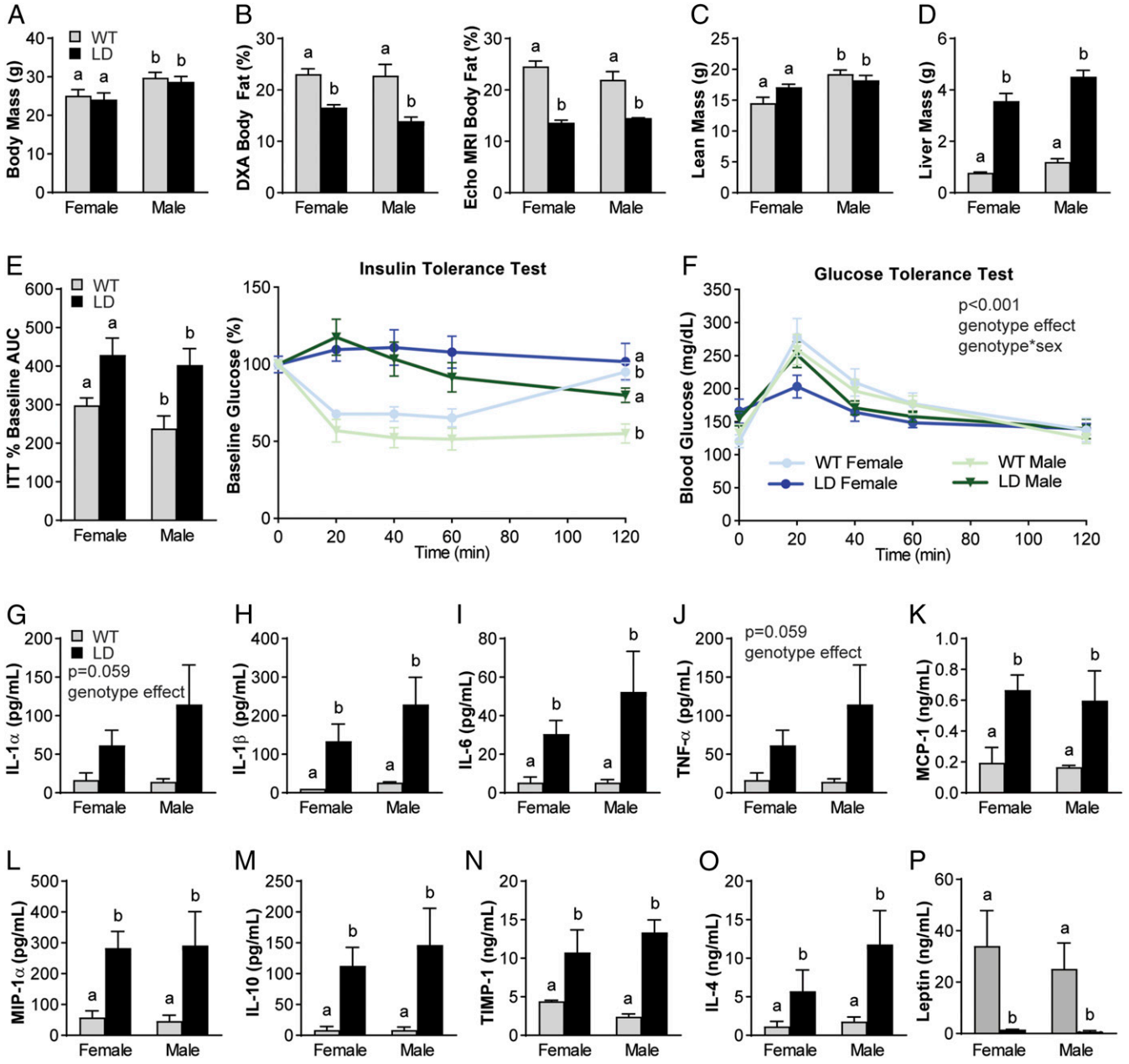

Fig. 1. Male and female LD mice demonstrate metabolic dysfunction and increased proinflammatory mediators in serum when compared to WT littermate controls. (*A–C*) LD mice have similar body mass (*A*) but decreased body fat when measured by DXA and Echo MRI (*B*) and similar lean mass (*C*) to same-sex WT littermates. (*D* and *E*) LD mice demonstrated increased liver mass (*D*), insulin-tolerance tests (*E*, *Right*), and AUC of insulin-tolerance tests (*E*, *Left*). (*F*) Glucose tolerance demonstrated a significant main effect of genotype and genotype × sex. (*G–O*) Regardless of sex, LD mice demonstrated increased serum proinflammatory (IL-1α, IL-1β, IL-6, TNF-α, MCP-1, MIP-1α) and increased antiinflammatory mediators (IL-10, TIMP-1, and IL-4) compared to WT littermate controls. (*P*) LD mice demonstrated near-zero levels of leptin in serum. $P < 0.05$ between groups is indicated by the letters "a" and "b" ($n = 7$ to 15 per group for *A–F*; $n = 3$ for female WT; $n = 4$ to 7 for other groups for *G–O* serum outcomes; analysis by two-way ANOVA with Sidak or Tukey's post hoc). ITT, insulin-tolerance test.

however, was significantly reduced in both LD and WT groups, as demonstrated in the time-course and AUC values (Fig. 4*E*). HFD did not further influence muscle weakness measured by forelimb grip strength in LD mice but did reduce grip strength in WT HFD-fed mice (Fig. 4*F*). Circulating leptin was increased in HFD-fed WT animals compared to chow-fed WT, but leptin remained undetectable in the serum of HFD-fed LD mice. (Fig. 4*G*). HFD did not result in increased circulating proinflammatory mediators in LD mice, as levels for IL-1α, IL-1β, IL-6, TNF-α, IP-10, and MCP-1 were similar to chow-fed LD levels (Fig. 4 *H–M*). IL-10 and IL-4 remained elevated in LD animals with HFD, whereas TIMP-1 was further elevated in HFD-fed LD mice, such that it was increased compared to both chow-fed LD mice and both WT groups (Fig. 4 *N–P*). For further differences in serum profiles, see *SI Appendix*, Table S1.

HFD-Fed LD Mice Are Protected from OA. HFD has been demonstrated to induce cartilage damage and OA in a manner that is exacerbated by joint trauma (2–9, 23). Thus, we examined if high-fat feeding could override the protection against joint damage

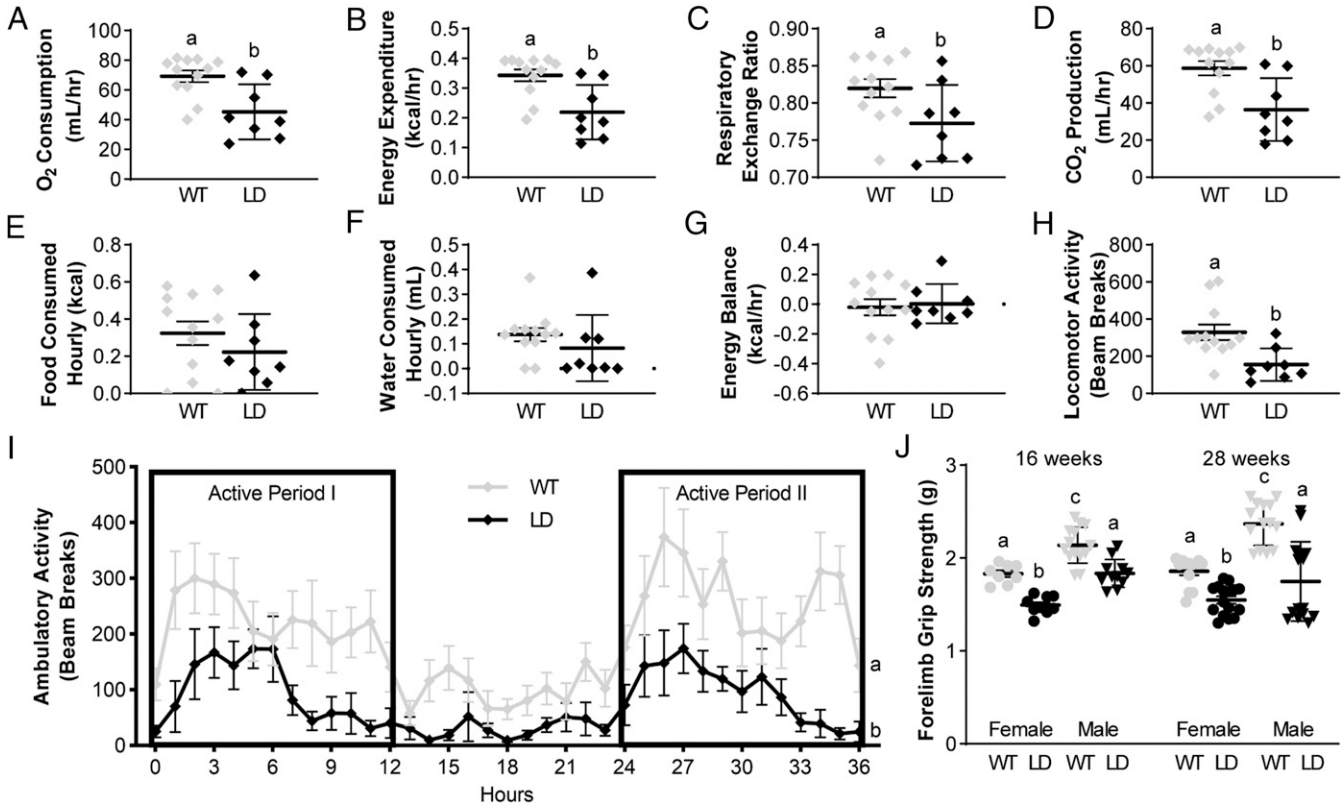

Fig. 2. LD mice fed a chow diet demonstrate reduced activity and muscle weakness, despite consuming similar amounts of food and water as WT controls. (*A–G*) Using indirect calorimetry, LD mice demonstrate reduced oxygen consumption (*A*), energy expenditure (*B*), respiratory exchange ratio (*C*), and CO_2 production (*D*) but similar hourly food (*E*), water (*F*), and overall average energy balance (*G*). (*H* and *I*) LD mice demonstrated lower locomotory (*H*) and ambulatory (*I*) activity. No differences were observed by sex, so data were pooled by genotype for comparison. (*J*) A sex-specific deficit in forelimb grip strength at 16 and 28 wk, operationalizing muscle strength, was observed in LD mice compared to WT controls. $P < 0.05$ between groups is indicated by the letters "a," "b," and "c" ($n = 7$ to 16 per group; *A–I*, general linear modeling using the CalR web-based tool; (*J*), three-way ANOVA with Dunnet's post hoc).

observed in chow-fed LD mice. Both male and female HFD-fed LD mice remained protected from OA as assessed by Modified Mankin Scores (Fig. 5 *A* and *B*). Both HFD-fed groups demonstrated significantly increased osteophyte scores in the DMM limbs (Fig. 5*C*). Synovitis scores were significantly increased in chow-fed LD DMM limbs as compared to contralateral control joints, and there was a trend toward a decrease in synovitis of HFD LD DMM limbs (Fig. 5*D*). Significant negative Pearson correlations were observed between serum levels of IL-10 ($r^2 = 0.42$; $P < 0.001$), TIMP-1 ($r^2 = 0.38$; $P < 0.001$), and IL-4 ($r^2 = 0.16$; $P < 0.035$) and Modified Mankin Scores of histological knee joint damage. No significant relations were observed between proinflammatory mediators like IL-6 ($r^2 = 0.06$; $P = 0.22$) and Modified Mankin Scores.

As with chow-fed animals, genotype was the principal driver of increased BMD and BV/TV in both the medial tibial plateau and the tibial metaphyses (Fig. 5 *E–G*), as well as the lateral tibial and femoral compartments (*SI Appendix*, Table S2). Medial tibial plateau BV/TV also showed a significant main effect of limb, and an interaction between limb × diet. Tibial metaphysis BV/TV demonstrated significant main effects of limb in addition to genotype, and significant interactions between limb × diet, limb × genotype, and limb × diet × genotype. For additional bone microstructure outcomes, see *SI Appendix*, Table S2.

LD animals fed chow and HFD were protected from hyperalgesia, as measured by the decreases in paw-withdrawal thresholds (Fig. 5*H*) and pressure-pain thresholds (Fig. 5*I*) observed in WT animals. Despite consistent increases in IL-10 in serum of LD mice on both diets, we did not observe changes in synovial fluid (SF) levels for IL-10 (Fig. 5*J*). In WT animals, HFD feeding was associated with increased SF TIMP-1 levels in the limb that underwent DMM (Fig. 5*K*). There were significant decreases in SF levels of leukemia inhibitory factor (LIF), TARC, and IL-12 (Fig. 5 *L–N*) in DMM limbs of LD mice. For SF profiles, see *SI Appendix*, Table S3.

Transplantation of Adipose Tissue Restores Susceptibility to OA in LD Mice. To determine if adipose tissue is a critical regulator of OA, we transplanted adipose tissue into chow-fed LD mice using two different methods. First, a mixture of subcutaneous and visceral adipose tissue from WT mice was implanted subcutaneously on the dorsum of LD mice (termed "WT fat-rescue"). A separate cohort received cell-based injections of primary mouse embryonic fibroblasts (MEFs) harvested from WT pregnant dams (termed "MEF-rescue"). MEF injections, delivered subcutaneously to the sternal aspect of mice, later regenerate a fat depot ~21 d post-injection, as previously described in this mouse model (18, 19).

Both groups of LD fat-transplant animals were challenged with DMM surgery, and histological assessment revealed that both WT fat-rescue and MEF-rescue animals demonstrated significant increases in DMM joint damage when compared to nonsurgical contralateral limbs. The severity of joint damage in either of the fat-rescue LD mice was similar to DMM damage in WT control animals (Fig. 6*A*), suggesting that fat implantation reintroduces susceptibility to cartilage damage in LD mice. Fat implant size was similar between groups (WT fat-rescue: 0.95 ± 0.1 g; MEF-rescue: 0.80 ± 0.07 g; $P = 0.18$), and mice receiving a fat implant maintained similar body mass with either WT fat-rescue (24.2 ± 0.7 g)

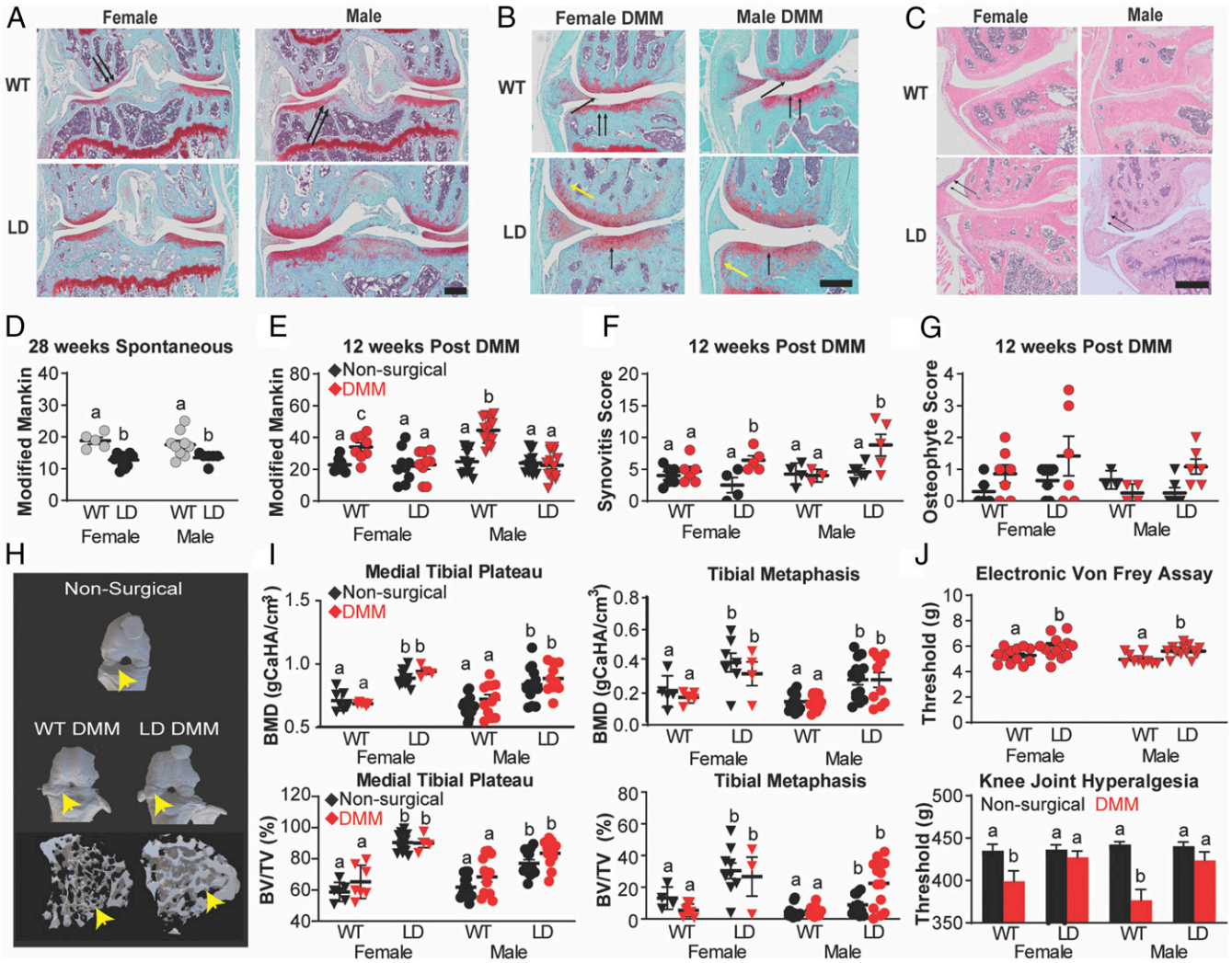

Fig. 3. LD mice are protected from spontaneous and posttraumatic OA. (*A*, *B*, *D*, and *E*) At 28 wk, both male and female LD mice demonstrated improvements in Modified Mankin Score (*A* and *D*) (black arrows indicate cartilage lesion) and, when challenged with DMM to induce posttraumatic OA, demonstrated similar scores to their contralateral nonsurgical limbs (*B* and *E*) (black indicates nonsurgical contralateral limb; red indicates DMM limb). (*B*, *C*, *F*, and *G*) LD male and female mice did demonstrate significant increases in synovitis post DMM (*C* and *F*) but similar osteophyte scores compared to WT controls. (*H*) 3D bone renderings of surface and morphology reveal that LD and WT DMM limbs demonstrate boney outgrowth around the medial meniscus and thicker trabeculae in LD mice at the tibial metaphysis (yellow arrows indicate areas of interest). (*I*) LD genotype drove increases in tibial plateau BMD and BV/TV, as well BMD and BV/TV in tibial metaphyses. (*J*) LD mice demonstrated protections from the onset of paw allodynia on the DMM limb, measured by Electronic Von Frey paw-withdrawal assay, and hyperalgesia at the knee, measured by SMALGO. Data were analyzed as two- or three-way ANOVA with either Sidak, Tukey's, or Dunnet post hoc ($n = 5$ to 15 per group). $P < 0.05$ between groups is indicated by the letters "a," "b," and "c." gCaHA/cm^3, grams of calcium hydroxyapatite per cubic centimeter. Scale bar indicates 100 μm.

or MEF-rescue (23.0 ± 0.2 g) mice as compared to the average body mass of chow-fed LD (26.3 ± 1.2 g; by one-way ANOVA: $P = 0.12$) mice. The size of the fat implant demonstrated a weak correlation with Modified Mankin Score ($r^2 = 0.22$; $P = 0.0176$) when both rescue groups were considered together. When analyzed separately, the size of WT fat-rescue implant size demonstrated no significant relationship with damage, while the MEF-rescue group demonstrated a strong significant relationship with implant size ($r^2 = 0.66$; $P < 0.001$) with Modified Mankin Score. Across all chow-fed animals, with and without transplant, there was no significant correlation between body mass and Modified Mankin Score ($r^2 = 0.028$; $P = 0.203$).

Osteophyte scores were only increased in MEF-rescue LD animals (Fig. 6*A*), while synovitis scores in the DMM limb were increased in the LD group compared to WT and were rescued to WT levels in the two transplant groups (Fig. 6*A*). Increases in BMD were reversed to WT levels in the medial tibial plateau of MEF-rescue LD animals, while BMD was similar in both limbs from WT fat-rescue animals to LD mice (Fig. 6*B*). Medial tibial plateau BV/TV was reversed to WT levels in MEF-rescue LD mice but only in the DMM limb of WT fat-rescue mice (Fig. 6*B*). Tibial metaphysis BMD was partially reversed to WT levels in MEF-rescue animals but similar to LD mice in WT fat-rescue mice (Fig. 6*B*). Tibial metaphysis BV/TV was reduced to WT levels in the DMM limbs of both fat-transplanted groups, while the nonsurgical contralateral limbs were similar to DMM limbs in LD mice (Fig. 6*B*). For lateral tibial plateau, medial femoral condyle, and lateral femoral condyle, as well as trabecular thickness and trabecular number data, see *SI Appendix*, Table S2.

Knee hyperalgesia in response to DMM was restored in WT fat-rescue and MEF-rescue LD animals to similar levels measured in WT DMM limbs (Fig. 6*C*), while DMM limb paw-withdrawal

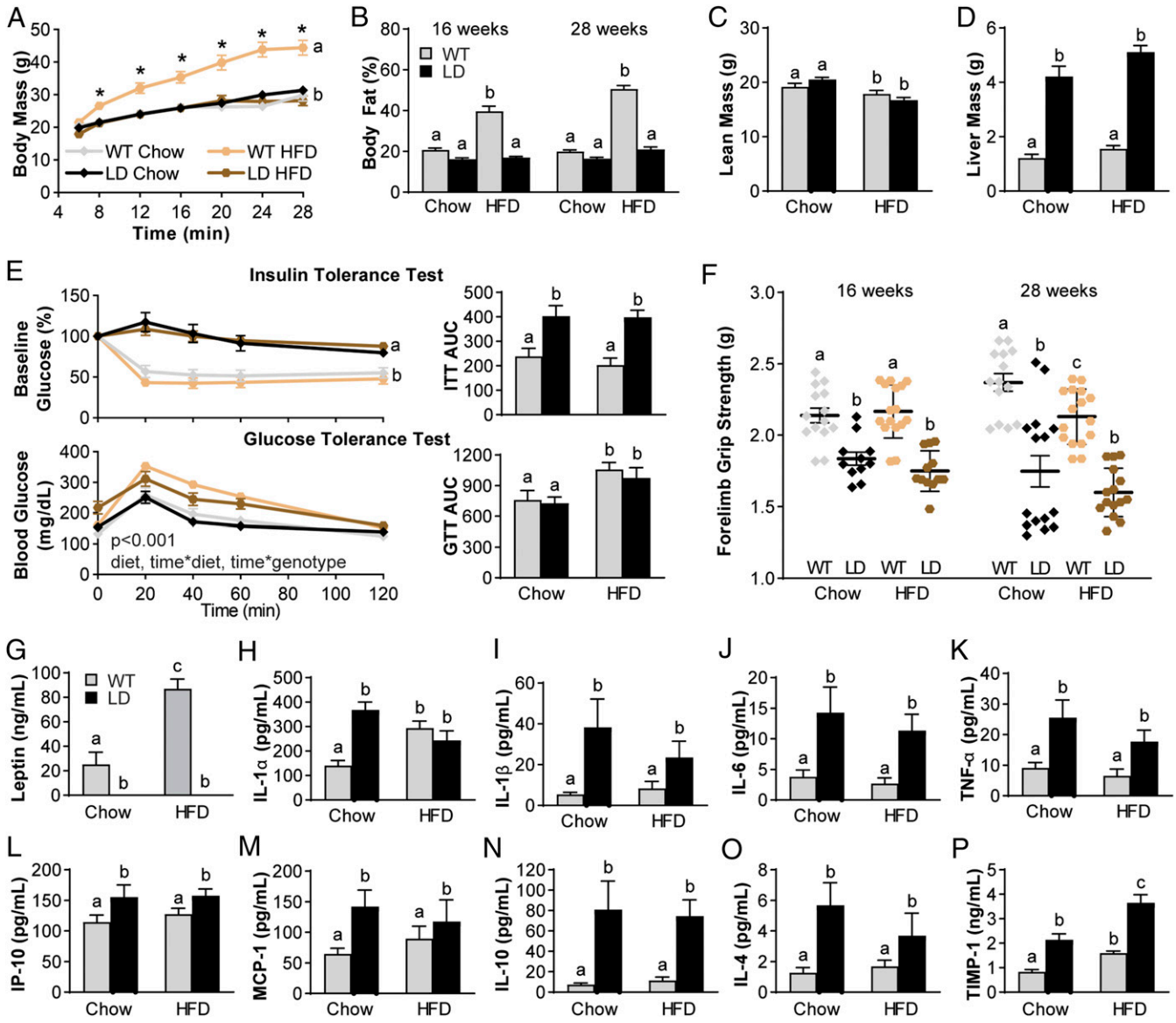

Fig. 4. HFD feeding of LD mice does not increase the metabolic derangement. (*A* and *B*) Body mass (*A*) and body fat (*B*) over time were only increased in WT animals fed HFD but not LD fed HFD. (*C* and *D*) Lean mass was decreased in both groups fed HFD (*C*), but liver mass was increased in LD mice to a similar extent even on HFD when compared to WT (*D*). (*E*) Insulin resistance by insulin-tolerance test was not affected by HFD, and differences were only observed by genotype, as in the AUC. Glucose sensitivity was reduced by HFD, as indicated in the AUC. (*F*) Muscle weakness was also decreased in LD mice and, at 28 wk, decreased in HFD-fed WT animals when compared to their 16-wk time point. (*G*) Serum leptin was increased in WT animals fed HFD but still completely absent in LD mice regardless of diet. (*H–M*) Levels of proinflammatory mediators that were elevated in LD mice were not further elevated by HFD (IL-1α, IL-1β, IL-6, TNF-α, IP-10, MCP-1). (*N–P*) Levels of antiinflammatory mediators IL-10 and IL-4 were similarly not increased by HFD in LD mice, but TIMP-1 was significantly increased. Data were analyzed as two- or three-way ANOVA with either Sidak, Tukey's, or Dunnet post hoc ($n = 10$ to 18 per group). $P < 0.05$ between groups is indicated by the letters "a," "b," and "c." GTT, glucose-tolerance test; ITT, insulin-tolerance test.

threshold remained similar in both fat-transplant groups to the values measured in LD animals (Fig. 6*C*). Forelimb grip strength was also restored in both WT fat-rescue and MEF-rescue animals (Fig. 6*C*).

Several aspects of the systemic metabolic profiles were improved in both MEF- and WT fat-rescue animals. Reduced locomotor activity was also reversed in both fat-transplant groups, such that both rescue groups showed activity profiles that were similar to WT animals and were significantly increased compared to LD animals (Fig. 6*D*). Insulin-tolerance curves were significantly reduced in both WT fat-rescue and MEF-rescue groups, but the AUC of these curves remained similar to the AUC of LD mice (Fig. 6 *E* and *F*). Glucose-tolerance curves were significantly improved in WT fat-rescue animals, but curves from MEF-rescue animals were similar to WT and LD animals (Fig. 6*G*). Serum leptin was restored in both MEF-rescue and WT fat-rescue LD mice, to ∼20 to 30% of endogenous circulating levels in WT mice (Fig. 6*H*).

Fat transplantation reduced the circulating levels of antiinflammatory mediators IL-10 and TIMP-1 in LD mice to WT levels (Fig. 6*I*). Proinflammatory mediators IL-6, TNF-α, and IL-1α were also reduced in WT fat-rescue and MEF-rescue animals, but IL-17 was significantly increased when compared to both LD and WT treated animals (Fig. 6*I*). Serum levels for IL-10 demonstrated a

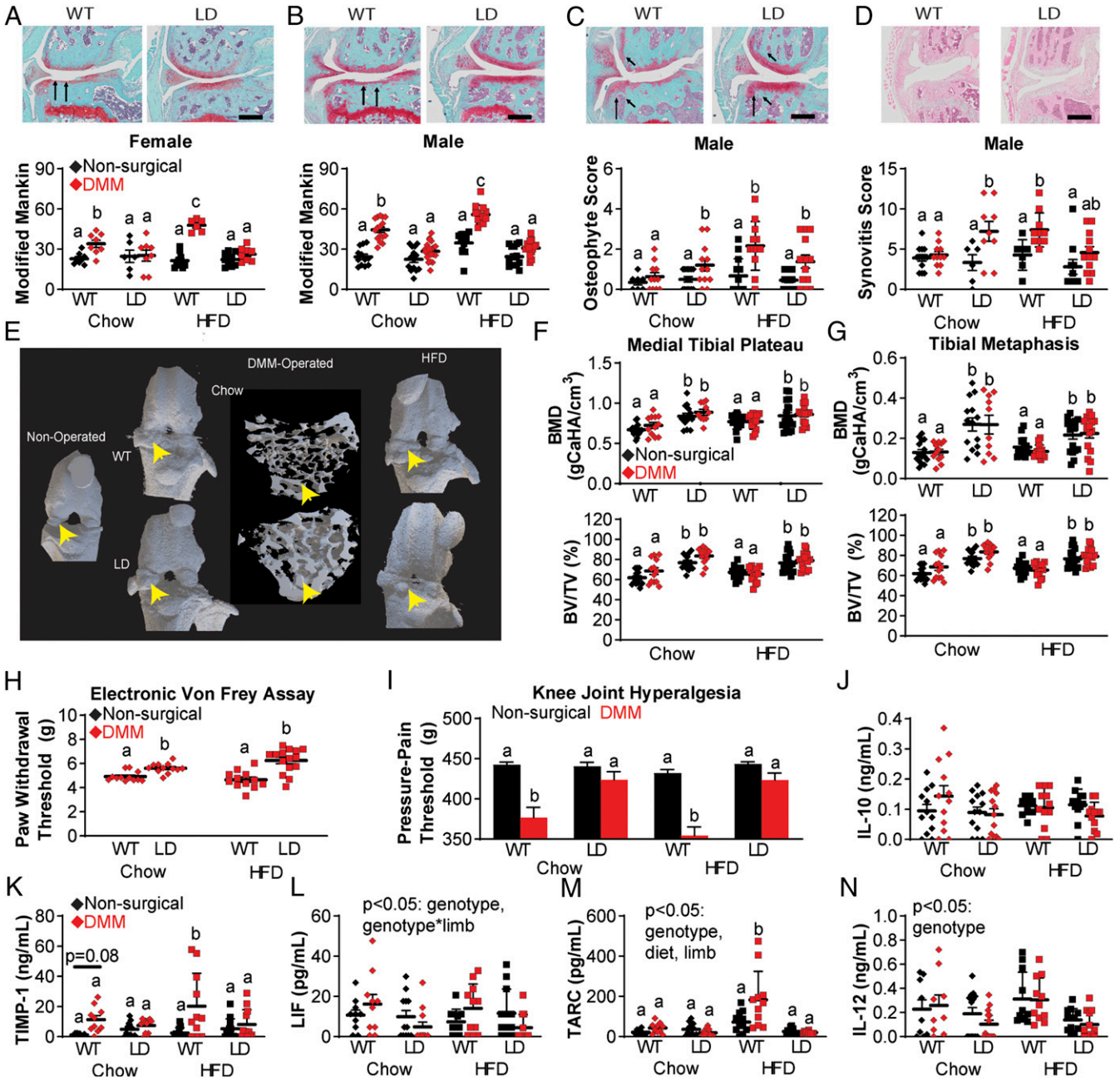

Fig. 5. HFD feeding does not override protection from posttraumatic OA in LD mice. (*A* and *B*) WT HFD-fed male and female animals demonstrated increased Modified Mankin Scores when compared to both chow WT DMM limbs and contralateral nonsurgical controls (black indicates nonsurgical contralateral limb; red indicates DMM limb). Regardless of diet or DMM surgery, LD mice demonstrated similar Modified Mankin Scores to their nonsurgical contralateral limbs. (*C*) HFD-fed LD mice did demonstrate a trend toward a reduction in synovitis in the DMM limb. (*D*) Both HFD WT and LD mice demonstrated increased osteophyte scores in the DMM limb. (*E*) 3D bone images from knee joint microCT and trabeculae from tibial metaphysis, bony outgrowth, and trabecular thickness (areas of interest indicated with yellow arrows). (*F* and *G*) Genotype drove the differences in BMD and BV/TV of medial tibial plateau and tibial metaphyses. (*H* and *I*) LD mice on both diets demonstrated protection from reduced paw-withdrawal threshold measured by Electronic Von Frey, and the onset of knee joint hyperalgesia measured by SMALGO, compared to WT controls in DMM limbs. (*J* and *K*) SF levels for antiinflammatory mediators IL-10 and TIMP-1 were similar by joint, genotype, and diet. (*L*–*N*) Reductions were observed in DMM LD joint SF levels for LIF and TARC. For remaining SF profiles, see *SI Appendix*. Data were analyzed as two- or three-way ANOVA with either Sidak, Tukey, or Dunnet post hoc tests ($n = 10$ to 18 per group). $P < 0.05$ between groups is indicated by the letters "a," "b," and "c." gCaHA/cm^3, grams of calcium hydroxyapatite per cubic centimeter. Scale bar indicates 100 μm.

modest, but significant, negative relationship with Modified Mankin Score when the fat-transplanted animals were included in the correlation analysis ($r^2 = 0.26$; $P < 0.001$). For serum differences due to fat transplantation, see *SI Appendix*, Table S4.

Despite the alterations we observed in the serum profiles of fat-transplant animals, we did not observe any differences in IL-10 concentration in the SF (Fig. 6*J*). SF levels for TIMP-1 in MEF-rescue animals were similar to those observed on contralateral and DMM limbs of WT mice; however, WT fat-rescue SF levels of TIMP-1 were decreased in both limbs, such that they were similar to the levels observed in the WT contralateral limb (Fig. 6*J*). Levels for IL-6 were significantly increased in both fat-transplant groups

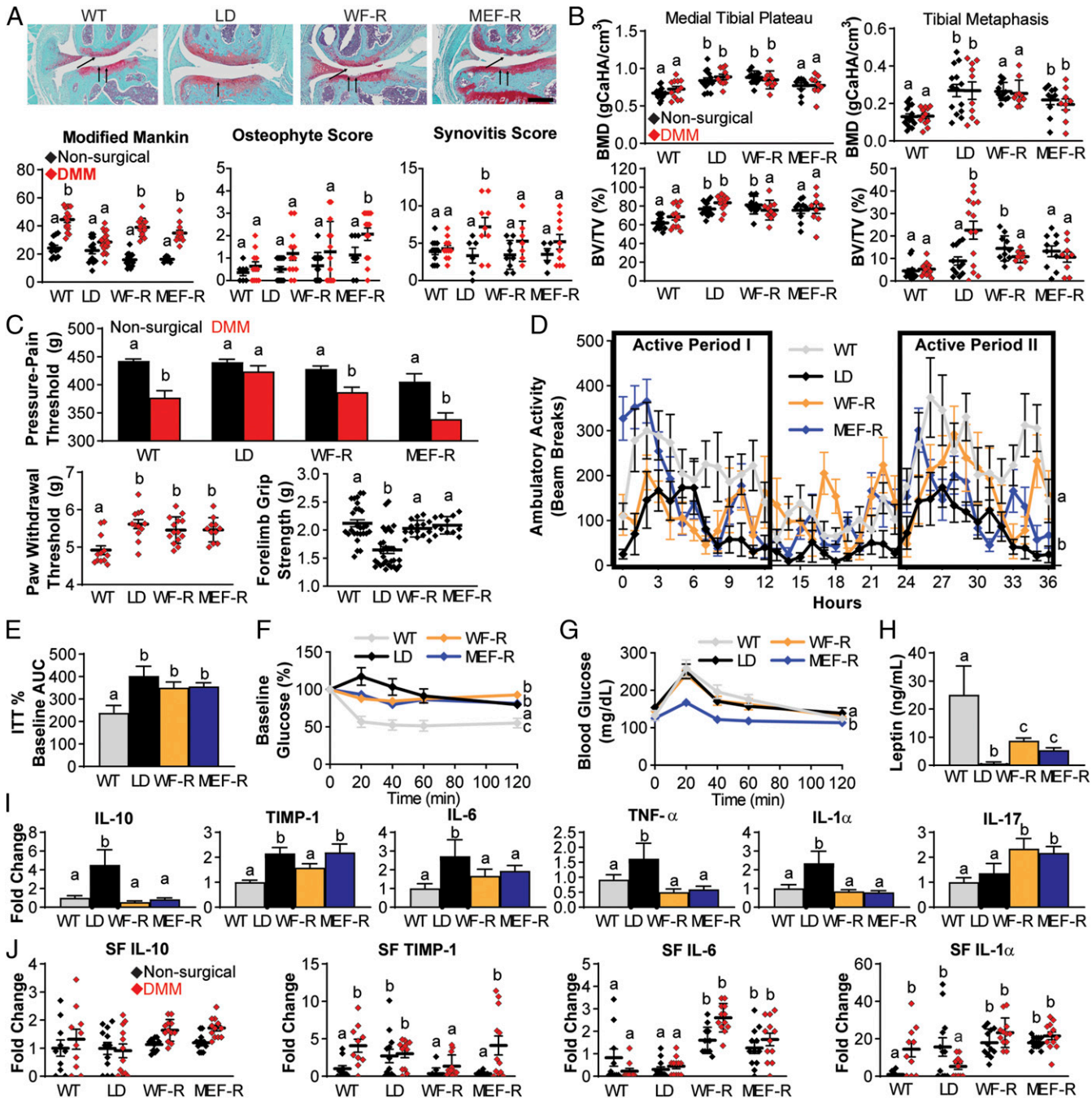

Fig. 6. Transplantation of fat restores susceptibility to OA damage and partially corrects the metabolic derangement in LD mice. (*A*) Both WT mature adipose (WF-R) transplant and primary mouse embryonic fibroblast (MEF-R) transplant in LD mice restores increased Modified Mankin Scores in DMM limbs (black arrows indicate areas of cartilage damage and proteoglycan loss; black symbols indicate nonsurgical contralateral limb, red symbols indicate DMM limb). Osteophyte scores were significantly increased in MEF-rescue animals compared to the other groups in DMM limbs. Synovitis scores were similar across groups in DMM limbs. (*B*) Medial plateau BMD and BV/TV in contralateral limb were reduced to WT levels in MEF-rescue animals only; WT fat-rescue animals' DMM limbs demonstrated significant reductions in BV/TV to WT levels. (*C*) Both transplant types restored susceptibility to knee hyperalgesia but not paw allodynia in the DMM limb; forelimb grip strength was also restored to WT levels in both transplant groups. (*D*) Restoration of activity levels was also observed in both transplant groups. (*E* and *F*) While both fat transplant groups demonstrated overall improvements in insulin resistance, the AUC was not significantly different from the LD mice. (*G*) WT fat-rescue, however, significantly improved glucose tolerance. (*H*) Leptin ELISA demonstrated that both fat transplant groups reintroduce circulating leptin levels to LD mice. (*I*) Serum levels for IL-10 were reduced in both transplant groups compared to LD mice, but serum TIMP-1 was only reduced in WT fat-rescue mice. Other proinflammatory mediators (IL-6, TNF-α, IL-1α) were also improved in transplant mice, whereas IL-17 was significantly elevated. (*J*) SF levels for IL-10 were similar across groups, whereas TIMP-1 levels in the DMM limbs were elevated to WT levels in MEF-rescue LD mice. SF levels for IL-6 and IL-1α were increased in WT fat-rescue and MEF-rescue animal DMM limbs. Data were analyzed as one-, two-, or three-way ANOVA with either Sidak, Tukey's, or Dunnet post hoc tests ($n = 7$ to 18 per group). $P < 0.05$ between groups is indicated by the letters "a," "b," and "c." gCaHA/cm^3, grams of calcium hydroxyapatite per cubic centimeter; ITT, insulin-tolerance test. Scale bar indicates 100 μm.

compared to LD and WT limbs, whereas SF IL-1α levels were decreased in LD DMM limbs but similarly increased in the limbs of both of WT fat-rescue and MEF-rescue LD animals (Fig. 6*J*). For a list of SF changes in WT fat-rescue and MEF-rescue animals, see *SI Appendix*, Table S5.

Discussion

While several studies have intimated relationships between adiposity, low-level systemic inflammation, and OA, the direct role of adipose tissue on cartilage health has been difficult to ascertain (1–4, 6–9, 22, 24–26). Herein, we demonstrate that knee joints from mice lacking adipose tissue are protected from spontaneous or injury-induced OA, even when fed a HFD. Because increased pain and hyperalgesia are the primary clinical symptoms of OA (27), we also assessed two pain-related outcomes: knee hyperalgesia and tactile allodynia, in addition to structural OA. We observed that LD mice are also protected from the onset of these pain-related outcomes with DMM, consistent with protection against structural damage. Remarkably, the transplantation of a small amount of adipose tissue mitigated or reversed these contributing factors (low-level systemic inflammation, metabolic disturbance, insulin resistance, sclerotic bone, muscle weakness, reduced activity) and restored susceptibility to cartilage damage and knee hyperalgesia in transplanted LD mice. Furthermore, these data support the notion that OA can be influenced and controlled by tissues outside of the joint organ system, as the addition of metabolically healthy fat can restore susceptibility in OA-resistant animals. This controlled model of LD confirms a direct relationship between adipose tissue and the onset and progression of OA, independent of biomechanical and metabolic contributors, although the specific factors involved in this protection remain to be clarified. Importantly, this model provides a system that will allow us to disentangle the contributions of specific adipokines to cartilage damage via this adipose–cartilage signaling axis.

The protection from cartilage damage observed in LD mice suggests that proinflammatory mediators released from adipose tissue could serve as therapeutic targets for OA. Adipose tissue may promote OA susceptibility directly through adipokine signaling, triggering systemic inflammation that ultimately manifests locally within the joint, although the exact mechanism by which this happens remains to be determined. Indeed, increased leptin levels have been consistently reported in obesity-induced OA (6, 7, 28, 29), potentially in response to leptin resistance (2), and may be responsible for driving OA-associated inflammation (29). Furthermore, leptin knockout mice are protected from OA (6, 7), consistent with the phenotype of LD mice in this study, which completely lack leptin. We observed that metabolic derangement and adipokine signaling can be rescued in the LD mice by the implantation of a surrogate fat pad derived from a MEF cell-based injection, or through mature adipose tissue implantation (5, 15), that restores between 20 to 30% of normal leptin levels in LD-transplanted mice. However, previous studies showed that inhibition of leptin failed to treat OA in the clinical setting, and directly exposing cartilage explants to leptin did not induce cartilage damage (6). Therefore, it is possible that the critical mediator involved in promoting OA in the LD mouse following fat transplant is downstream of leptin. Ongoing studies will further elucidate the specific role of this adipokine.

LD mice demonstrate consistently higher serum levels of proinflammatory mediators (e.g., IL-1α, IL-1β, IL-6, TNF-α, MCP-1, IP-10). We speculate that increased proinflammatory mediator levels are related to the hepatic steatosis pathology (30), which has previously been observed in LD mice (12), that is also observed in the present study via the large increases in liver mass in LD mice. We postulate that the strong proinflammatory profiles in LD mice can help separate the contribution of adipokines from other mediators related to metabolic disturbance or liver pathology in this context. Our future efforts hope to determine the exact contribution of liver pathology to these serum inflammatory profiles.

LD mice, however, also demonstrate high levels of various antiinflammatory mediators (IL-10, TIMP-1, IL-4). IL-10, a potent antiinflammatory molecule that is negatively associated with cartilage damage, has been proposed as an OA therapeutic and pain reliever (31, 32). Due to structural homology, IL-10 can substitute for leptin (33) and reduces insulin resistance and HFD-induced inflammation in models of obesity without off-target proinflammatory consequences (34). In fat- or MEF-rescue LD mice, we saw a decrease in circulating serum levels of IL-10, which could potentially explain the reversal of cartilage protection observed in nontransplanted LD mice. IL-10 is known to induce TIMP-1 and reduce the activity of matrix metalloproteinases (35). IL-10 may drive the increases in TIMP-1 seen in serum and SF of LD mice. However, increases in TIMP-1 alone does not protect against OA phenotype. Future work will determine if sustained increases in circulating levels of IL-10 is indeed a key protective mechanism against cartilage damage in LD mice.

Adipose transplantation increased circulating levels of IL-17, an inflammatory cytokine previously implicated in OA pathogenesis (36). IL-17 has been shown to regulate adipogenesis, glucose homeostasis, and obesity (37). Whether fat or MEF transplant directly produces IL-17 or, more likely, stimulates IL-17 production from host cells (38) remains to be determined. However, studies have previously shown that the MEFs delivered as a cell-based therapy ultimately form a tissue that integrates well into the host (18, 19). Thus, the IL-17 increases observed in MEF-rescue and WT fat-rescue animals may reflect the integration and lipid storage that results from implantation in LD mice. Ultimately, IL-17 could be a key factor contributing to the restoration of OA susceptibility in LD mice upon fat transplant, as others have reported IL-17 as a potential biomarker for a distinct subset of inflammatory OA patients with end-stage disease (39).

It is important to note that LD mice also lack other signaling molecules, such as adipsin, or complement factor D, which cleaves factor B to initiate alternative complement-pathway activity (12). Previous studies have demonstrated a protective effect of adipsin deficiency on both spontaneous and posttraumatic OA pathogenesis (15, 40), so it is unclear whether adipsin deficiency protects against joint damage in the present studies. Our ongoing work is interrogating the role of adipsin-knockout animals in the presence of HFD and OA to determine if the absence of adipsin signaling in particular protects against cartilage damage in the LD mouse.

Synovitis has been associated previously with HFD-induced OA (5, 8, 9, 22, 41). Here, we observed increased synovitis in LD mice, in addition to several differences in SF cytokine concentrations that are generally consistent with OA pathogenesis (36). However, we did not observe overt structural damage to LD knee joint cartilage in these mice, suggesting that the factors driving synovial inflammation are separable from those driving changes in cartilage structure and loss in OA. Specifically, in SF, we observe reduced levels for LIF and IL-12 in the DMM limbs of LD mice and a concordant increase in IL-1α and IL-6 in MEF-rescue and WT fat-rescue LD mice. This implicates a role for the IL-1 and IL-6/IL-12 family of cytokines in protection and susceptibility to OA, which have been postulated as key therapeutic target networks for OA (36). Notably, we did not see a reversal of synovitis in MEF-rescue and WT-fat rescue animals, which may be either contributing to or in response to this increase in SF IL-1α and IL-6. Moreover, we observed decreased levels for TARC/CCL-17 in LD DMM limbs, which is of interest as CCL-17 blockade has been demonstrated as a therapeutic candidate for OA structure and pain (42). In the fat-rescue groups, we observed increased circulating levels of TARC/CCL-17 but decreased SF levels for TARC/CCL-17. IL-4 is another promising antiinflammatory candidate for cartilage protection under active investigation, and,

here, we observed increased IL-4 in LD mice (43). However, as IL-4 can also induce TARC/CCL-17 via STAT6, this may offset the therapeutic effect of IL-4 overexpression (44). Future studies will evaluate the direct influence of IL-6/IL12 axis and TARC/CCL-17 signaling in the protection from OA in LD mice.

A striking absence of antiinflammatory signatures were found in the SF of LD mice when compared to WT mice, which may also be consistent with the increased synovitis we observed in LD mice. There are a few plausible explanations for this finding. First, evaluating data cross-sectionally at the terminal end point of 12 wk post-DMM does not allow for temporal assessment of changes in the systemic or local inflammatory environment, and it is possible that critical changes in the SF that contribute to cartilage protection occur soon after DMM and are not detectable at the terminal end point. A second possibility is that the systemic environment, which is directly affected by the absence and implantation of adipose tissue, is mitigating and driving OA disease pathogenesis in this LD model system. This proposition is consistent with several studies that demonstrate increased body mass per se does not explain obesity-associated knee OA but that, in fact, associations with systemic proinflammatory mediators and other tissues (e.g., muscle) provide robust associations with OA pathogenesis (1, 4, 6, 7, 28, 29), which is the opposite of what we observed in the LD mice. As such, we postulate that the strong antiinflammatory signature evidenced in LD mice, which is reversed upon adipose implantation, is a key driver of this protection and that systemic overexpression of antiinflammatory mediators may be a useful therapeutic approach for chondroprotection with injury or obesity. However, it is important to note that the source of these cytokines may influence their effect on joint tissues. For example, it has been hypothesized that the infrapatellar fat pad, which is absent in LD mice, may serve as a local source of intraarticular adipokines mediating knee OA (26, 28). In addition, many of the proinflammatory mediators that are increased in LD mice can be produced in other tissues, such as the liver, which shows increased size and pathology in this model (12). Increased liver fat is associated with increased circulating levels of proinflammatory mediators in serum (45), including IL-6, even when adjusted for BMI and visceral fat content. Further work is needed to determine the specific signals and mediators secreted from adipose tissue that drive OA pathogenesis.

An important finding in these studies is the remarkable presence of bone sclerosis in concordance with healthy cartilage in LD mice, which was subsequently reversed with fat transplantation. Many studies have hypothesized that subchondral sclerosis is a pathological characteristic of and key contributor to OA (11, 20), even proposing that subchondral bone remodeling is a primary driver of cartilage damage (20). However, our findings clearly demonstrate that these factors are biologically separable, and healthy cartilage can persist even when challenged with trauma, in the presence of marked subchondral sclerosis and increased bone density throughout the joint. Similarly, the reversal of muscle weakness observed in LD mice with fat implantation contradicts many studies that have suggested a key role for muscle weakness in the pathogenesis of OA (2, 8). This includes recent work from our laboratory that demonstrates risk for posttraumatic OA can be mitigated by enhancing muscle structure and strength and correcting metabolic derangement using a gene therapy approach (5). Future studies will aim to resolve these issues and disentangle these risk factors for obesity and OA using the LD mouse platform and time-course studies. These insights may contribute to our evolving understanding of mechanical and biological tissue cross-talk, both within and between the joint organ system, including whether cartilage can feed back and signal to adipose tissue. These lines of inquiry will help determine what constitutes compensatory versus pathological loading and inflammatory environments. Using this insight, we can begin to unravel intrinsic mechanisms that other tissues of the joint organ system or other tissues external to the joint may employ in efforts to protect cartilage in situations of trauma or challenge. These data can facilitate clarity around critical drivers, likely derived from adipose tissue, which may be foundational in the onset of obesity- or joint injury-induced OA as well as form the basis for novel therapeutic strategies.

LD mice showed reduced activity as compared to the WT mice, and this phenotype was reversed by fat transplantation. While the relationship between OA and activity is complex, we and others have found that increased joint loading due to exercise is protective against joint damage with obesity (46–48). However, we also observed decreased muscle strength in LD mice, prior to DMM surgery, which is strongly related to decreased activity and widely implicated in OA onset and progression (2), but observe cartilage protection in LD mice. Another recent study in our laboratory demonstrated that protection of muscle strength and function using systemic overexpression of follistatin via gene therapy protected mice from HFD-induced cartilage damage with DMM (5). These findings indicate the complex interplay among muscle strength, activity, adipose signaling, and joint loading in the context of OA, which can hopefully be addressed in future studies using this model.

Conclusion

Adipose tissue is a critical antagonist of cartilage health and integrity independent of body mass, systemic inflammation, synovitis, muscle weakness, and subchondral bone sclerosis. Specifically, these data implicate several context-relevant therapeutic targets: a joint/cartilage protective role conferred by systemic increases in IL-10 and TIMP-1 or inhibition of IL-6/IL-12, leptin, IL-17, and CCL-17 axes. Characterizing adipose–cartilage cross-talk and signaling may lead to novel therapeutic opportunities for OA as well as other metabolic diseases involving adipose dysfunction. The LD mouse provides a powerful tool to disentangle the mechanisms involved in cartilage protection and vulnerability, and our ongoing efforts aim to clarify these mechanisms by interrogating specific adipokines/cytokines identified in the present study.

Materials and Methods

Animals and Design. All experimental procedures were approved by the Institutional Animal Care and Use Committee and were carried out in accordance with the guidelines prescribed by the Washington University School of Medicine Department of Comparative Medicine. LD mice and WT littermate controls were developed by crossing adiponectin-Cre mice with homozygous lox-stop-lox-ROSA-diphtheria toxin A mice on a C56BL/6 background (1) and were maintained at thermoneutrality throughout their lifespan (30 °C). Male and female offspring were weaned at 4 wk of age to either a chow diet (13% fat; 29% protein; 60% carbohydrate; energy density, 3.0 kcal/g) (standard chow) or HFD (60% fat; 20% protein; 20% carbohydrate; energy density, 5.2 kcal/g) (D12492; Research Diets) ad libitum through 28 wk of age (n = 7 to 16 per group). Mice were group-housed such that n = 3 to 5 per cage, and genotypes were mixed within a given cage. For the timeline of these studies, see *SI Appendix*, Fig. S1. In the transplantation studies, male and female LD mice received either a MEF transplant (MEF-rescue) (19), between 3 and 5 wk of age, or WT fat transplant containing visceral and subcutaneous fat (WT fat-rescue) (16, 17), between 6 and 8 wk of age. At 16 wk, surgical animals underwent surgery for DMM in their left knee joints, and the right limb served as a nonsurgical contralateral control (5, 8, 9, 49). Behavioral and metabolic assays were conducted throughout the course of this study. Mice were sacrificed at 28 wk of age to assess OA severity, bone microstructure, and serum and SF inflammatory profiles.

Body Weight and Composition. Mice were weighed weekly throughout the course of the study. Body fat was measured by DXA (Lunar Piximus) at 15 and 27 wk of age. In a subset of animals, an Echo MRI 3-in-1 instrument (Echo Medical Systems) was used to quantify body fat.

Fat Transplantation. MEFs were harvested from E14 C57BL/6J embryos, resuspended in phosphate-buffered saline (PBS), and delivered as a subcutaneous

injection on the sternal aspect of the animals, as described previously (19). Embryos were isolated immediately after the pregnant dams were cervically dislocated. The liver, heart, and intestine were removed from decapitated embryos, and the remaining tissue was minced and digested in 1.25 mL of 0.05% trypsin for 45 min in a 37 °C water bath. Trypsin was neutralized with a mixture of Dulbecco's Modified Eagle medium, 1% penicillin-streptomycin, and 10% fetal bovine serum, triturated vigorously by pipetting up and down ∼30 times, and filtered using a 70-μm cell strainer. The filtrate was then centrifuged at 500 × *g* for 6 min, and the cell pellet was resuspended in 250 μL of PBS. The injection was delivered using a 27-gauge insulin syringe into a donor LD mouse that was 3 to 5 wk old and anesthetized under 2 to 3% isoflurane.

Mature fat depots were implanted in accordance with previously described methods (16, 17). Donor WT mice (6 to 8 wk old) were euthanized, and subcutaneous and visceral fat pads were harvested and cut into 100- to 150-mg pieces, in PBS on ice. Recipient mice were anesthetized using 2 to 3% isoflurane, dorsal hair was shaved, fat was implanted (∼1 g/mouse), and incisions were closed with absorbable sutures.

Posttraumatic OA Induction by DMM. At 16 wk of age, mice were challenged with unilateral DMM on their left knee joint, in accordance with previously described methods (9, 49). Briefly, anesthetized mice were positioned supine in a custom-designed device that maintained 90° of knee flexion in the left knee. The medial meniscotibial ligament was approached from the medial aspect of the knee by creating a small incision in the skin, followed by an incision in the joint capsule, and ultimately transected. The joint capsule and skin were closed by absorbable sutures and Vetbond (3M, Inc.) skin glue.

Histological Assessment of OA, Synovitis, and Osteophytes. At 28 wk of age, 12 wk post-DMM surgery, mice were euthanized and knee joints were assessed using histology. Knee joints were harvested, and all excess tissue and muscle were trimmed and fixed in 4% paraformaldehyde for 24 h. Limbs were decalcified in 10% formic acid (Cal-Ex) for 72 h, dehydrated, processed, and embedded in paraffin blocks. Serial frontal plane sections were cut at 5 μm and stained with either hematoxylin, fast green, and safranin O (saf-O/fast green) or hematoxylin and eosin (H&E). Saf-O/fast green slides were scored using Modified Mankin Criteria to operationalize knee joint damage (5, 9). This scoring system employs a 30-point scale for four compartments of the frontal plane section (medial tibial plateau, lateral tibial plateau, medial femoral condyle, lateral femoral condyle), which is added to generate the total Modified Mankin Score for a joint that serves as the semiquantitative measure for joint damage. To assess synovitis in these joints, H&E-stained slides were graded for synovial stroma density (0 to 3) and synovial lining thickness (0 to 3) for all four compartments of the synovium in the joint, corresponding to the four regions assessed in the Mankin Score. These values were summed to provide a total semiquantitative measure of synovitis (5, 9). Finally, to determine whole joint osteophytosis, the same four quadrants of each knee joint were graded from 0 to 3 using previously described methods (9) and summed for a cumulative score per joint. All histological scores represent the average values from scores of three blinded graders, and the interrater reliability measured by intraclass correlation was $r > 0.90$ ($P < 0.001$).

Bone Microstructural Analysis. Whole knee joints were scanned by microcomputed tomography (Bruker SkyScan1176) at a resolution of 18-μm isotropic voxel resolution according to previously reported methods (5, 8). To reduce beam hardening, a 0.5-mm aluminum filter was used during scanning. Hydroxyapatite calibration phantoms were scanned to calibrate bone density. Scans were reconstructed to three-dimensional (3D) images using NRecon software, and CTAn software was used to segment subchondral and trabecular regions from the medial tibial plateau, lateral tibial plateau, medial femoral condyle, and lateral femoral condyle for analysis. The tibial epiphysis was identified using the subchondral plate and growth plate as references. The tibial metaphysis was defined as the 1-mm area directly below the growth plate. The main outcomes reported from microCT images are BMD, BV/TV (%), trabecular number, and trabecular thickness.

Serum and SF Profiling. All mice were fasted prior to sacrifice. Serum was collected in a serum separator tube and allowed to clot at room temperature. SF was collected using an alginate pad that was digested in alginate lyase until a stop solution was applied (5, 8). Both fluids were stored at −80 °C until analysis by Luminex multiplex 44-plex chemokine/cytokine array assay (Eve Technologies). The 44-plex assay included eotaxin, erythropoietin, 6Ckine, fractalkine, G-CSF, GM-CSF, IFNB1, IFNγ, IL-1α, IL-1β, IL-2, IL-3, IL-4, IL-5, IL-6, IL-7, IL-9, IL-10, IL-11, IL-12 (p40), IL-12 (p70), IL-13, IL-15, IL-16, IL-17, IL-20, IP-10, KC, LIF, LIX, MCP-1, MCP-5, M-CSF, MDC, MIG, MIP-1α, MIP-1β, MIP-2, MIP-3α, MIP-3B, RANTES, TARC, TIMP-1, TNF-α, and VEGF. Serum was assessed at a dilution of 1:2, and SF was evaluated at a dilution of 1:75 based on the minimum concentration of 75 μL.

Enzyme-linked immunosorbent assay (ELISA) for serum leptin was conducted using a mouse/rat Leptin Quantikine ELISA Assay kit (MOB00; R&D Systems) at a dilution of 1:2 in LD mice, and all other groups were evaluated at the manufacturer's recommended 1:20 dilution. The lower limit of detection of the assay was 22 pg/mL, and the interassay variability was 3 to 4%.

Insulin- and Glucose-Tolerance Tests. Insulin- and glucose-tolerance tests were performed 4 wk post-DMM surgery (20 wk of age) after fasting mice for a minimum of 4 h. Each test was conducted at least 1 wk apart in all animals. For both tests, fasting glucose levels were measured by tail bleed at time point 0 to establish a baseline. For glucose-tolerance tests, animals were administered 1 mg/kg (10% dextrose: 1% volume/body mass) by intraperitoneal (IP) injection, and for insulin-tolerance tests, 0.75 U/kg body mass of insulin (Humulin R diluted to 75 mU/mL, 1% volume/body mass) was administered by IP injection (19). Serial blood glucose measurements were taken via tail vein at 20, 40, 60, and 120 min after injection with a glucose meter (Contour; Bayer).

Metabolic Parameters. Indirect calorimetry and activity were measured over 36 h after a 6-h acclimatization period using a Phenomaster (TSE Systems) Metabolic Caging System at room temperature (22 °C) at 22 to 24 wk of age. Each mouse was individually housed during the observation period and given free access to food and water. Data were analyzed using the CalR web-based tool for indirect calorimetry experiments (50) using the two-group or four-group templates and one-way ANOVA with Tukey's post hoc test.

Pain-Related Assessments and Behavioral Testing. All animals were acclimatized to all equipment 1 d prior to the onset of testing. Forelimb grip strength was used to measure muscle strength both prior to DMM at 15 wk of age and, prior to sacrifice at 27 wk of age, using a Chatillon DFE Digital Force Gauge (Johnson Scale Co.). Each mouse was evaluated five times with a minimal resting period of 90 s between trials, and these trials were averaged to determine the grip-strength value for each mouse. Two measures for pain were conducted at 27 wk of age. To assess tactile allodynia in the DMM limb, an Electronic Von Frey assay was used. Mice were placed individually in acrylic cages (12 × 10 × 17 cm high) with a wire grid floor. Hind paws of DMM limbs were stimulated two to three times. A hand-held force transducer with a 0.5-mm 2-polypropylene tip (Electronic Von Frey anesthesiometer; IITC Life Sciences) was used to apply force against the central aspect of the DMM hind paw. The intensity of the stimulus (grams) was recorded by the tester when the paw was withdrawn. The stimulation of the paw was repeated until the animal presented three similar measurements. To assess mechanical hyperalgesia, pressure-pain tests were conducted using a Small Animal Algometer (SMALGO) (Bioseb) (5). Three trials of the surgical and nonsurgical limb were collected by applying a steadily increasing force to the lateral aspect of each limb until the limb was withdrawn. The average of three trials for each limb was reported, and maximum value of 450 g was employed to avoid tissue damage to the knee joint.

Statistical Analysis. Statistical analysis and number of animals per group for each experiment are described in each figure legend. Analysis was performed in Graphpad Prism 8 (Graphpad Software) or SPSS Statistics 23 (IBM). A priori α was defined as 0.05. Data are presented as means ± SE and were compared by either one-way, two-way (group × limb; genotype × sex; genotype × diet), or three-way (limb × genotype × diet; limb × genotype × sex) ANOVA with Dunnet, Sidak, or Tukey's post hoc test.

Data Availability. All data needed to evaluate the conclusions in the paper are present in the article and *SI Appendix*.

ACKNOWLEDGMENTS. We thank Natalie Kelly and Erica Ely for assistance with behavior-testing experiments and Sara Oswald for assistance with editing and figure composition. This work was funded by the Shriners Hospitals for Children, Musculoskeletal Research Center Pilot Grant P30 AR074992, and Feasibility and Just-In-Time Grant Program Grants T32 DK108742 and T32 DK007120. This study was supported, in part, by NIH Grants AR50245, AG15768, AG46927, AR076820, AR073752, and OD10707; the Arthritis Foundation; and the Nancy Taylor Foundation for Chronic Diseases.

1. F. Berenbaum, T. M. Griffin, R. Liu-Bryan, Review: Metabolic regulation of inflammation in osteoarthritis. *Arthritis Rheumatol.* **69**, 9–21 (2017).
2. K. H. Collins *et al*., Obesity, metabolic syndrome, and musculoskeletal disease: Common inflammatory pathways suggest a central role for loss of muscle integrity. *Front. Physiol.* **9**, 112 (2018).
3. K. H. Collins *et al*., Relationship between inflammation, the gut microbiota, and metabolic osteoarthritis development: Studies in a rat model. *Osteoarthritis Cartilage* **23**, 1989–1998 (2015).
4. K. H. Collins, R. A. Reimer, R. A. Seerattan, T. R. Leonard, W. Herzog, Using diet-induced obesity to understand a metabolic subtype of osteoarthritis in rats. *Osteoarthritis Cartilage* **23**, 957–965 (2015).
5. R. Tang *et al*., Gene therapy for follistatin mitigates systemic metabolic inflammation and post-traumatic arthritis in high-fat diet-induced obesity. *Sci. Adv.* **6**, eaaz7492 (2020).
6. T. M. Griffin *et al*., Diet-induced obesity differentially regulates behavioral, biomechanical, and molecular risk factors for osteoarthritis in mice. *Arthritis Res. Ther.* **12**, R130 (2010).
7. T. M. Griffin, J. L. Huebner, V. B. Kraus, F. Guilak, Extreme obesity due to impaired leptin signaling in mice does not cause knee osteoarthritis. *Arthritis Rheum.* **60**, 2935–2944 (2009).
8. N. S. Harasymowicz *et al*., Intergenerational transmission of diet-induced obesity, metabolic imbalance, and osteoarthritis in mice. *Arthritis Rheumatol.* **72**, 632–644 (2020).
9. C. L. Wu *et al*., Dietary fatty acid content regulates wound repair and the pathogenesis of osteoarthritis following joint injury. *Ann. Rheum. Dis.* **74**, 2076–2083 (2015).
10. P. Y. Mengsteab *et al*., Mechanically superior matrices promote osteointegration and regeneration of anterior cruciate ligament tissue in rabbits. *Proc. Natl. Acad. Sci. U.S.A.* **117**, 28655–28666 (2020).
11. E. Thijssen, A. van Caam, P. M. van der Kraan, Obesity and osteoarthritis, more than just wear and tear: Pivotal roles for inflamed adipose tissue and dyslipidaemia in obesity-induced osteoarthritis. *Rheumatology (Oxford)* **54**, 588–600 (2015).
12. X. Wu *et al*., Contribution of adipose-derived factor D/adipsin to complement alternative pathway activation: Lessons from lipodystrophy. *J. Immunol.* **200**, 2786–2797 (2018).
13. C. Xie, Q. Chen, Adipokines: New therapeutic target for osteoarthritis? *Curr. Rheumatol. Rep.* **21**, 71 (2019).
14. J. Chang *et al*., Systemic and local adipose tissue in knee osteoarthritis. *Osteoarthritis Cartilage* **26**, 864–871 (2018).
15. G. Valverde-Franco *et al*., High in vivo levels of adipsin lead to increased knee tissue degradation in osteoarthritis: Data from humans and animal models. *Rheumatology (Oxford)* **57**, 1851–1860 (2018).
16. W. Zou *et al*., Congenital lipodystrophy induces severe osteosclerosis. *PLoS Genet.* **15**, e1008244 (2019).
17. Y. Li *et al*., Fat-produced adipsin regulates inflammatory arthritis. *Cell Rep.* **27**, 2809.e3–2816.e3 (2019).
18. A. Brenot, I. Hutson, C. Harris, Epithelial-adipocyte interactions are required for mammary gland development, but not for milk production or fertility. *Dev. Biol.* **458**, 153–163 (2020).
19. D. Ferguson, M. Blenden, I. Hutson, Y. Du, C. A. Harris, Mouse embryonic fibroblasts protect ob/ob mice from obesity and metabolic complications. *Endocrinology* **159**, 3275–3286 (2018).
20. D. B. Burr, E. L. Radin, Microfractures and microcracks in subchondral bone: Are they relevant to osteoarthrosis? *Rheum. Dis. Clin. North Am.* **29**, 675–685 (2003).
21. K. H. Collins *et al*., Association of metabolic markers with self-reported osteoarthritis among middle-aged BMI-defined non-obese individuals: A cross-sectional study. *BMC Obes.* **5**, 23 (2018).
22. C. L. Wu, K. A. Kimmerling, D. Little, F. Guilak, Serum and synovial fluid lipidomic profiles predict obesity-associated osteoarthritis, synovitis, and wound repair. *Sci. Rep.* **7**, 44315 (2017).
23. C. L. Wu *et al*., Conditional macrophage depletion increases inflammation and does not inhibit the development of osteoarthritis in obese macrophage fas-induced apoptosis-transgenic mice. *Arthritis Rheumatol.* **69**, 1772–1783 (2017).
24. C. L. Wu, N. S. Harasymowicz, M. A. Klimak, K. H. Collins, F. Guilak, The role of macrophages in osteoarthritis and cartilage repair. *Osteoarthritis Cartilage* **28**, 544–554 (2020).
25. D. Hamada *et al*., Suppressive effects of insulin on tumor necrosis factor-dependent early osteoarthritic changes associated with obesity and type 2 diabetes mellitus. *Arthritis Rheumatol.* **68**, 1392–1402 (2016).
26. N. S. Harasymowicz *et al*., Regional differences between perisynovial and infrapatellar adipose tissue depots and their response to class II and class III obesity in patients with osteoarthritis. *Arthritis Rheumatol.* **69**, 1396–1406 (2017).
27. D. Syx, P. B. Tran, R. E. Miller, A. M. Malfait, Peripheral mechanisms contributing to osteoarthritis pain. *Curr. Rheumatol. Rep.* **20**, 9 (2018).
28. E. Barboza *et al*., Profibrotic infrapatellar fat pad remodeling without M1 macrophage polarization precedes knee osteoarthritis in mice with diet-induced obesity. *Arthritis Rheumatol.* **69**, 1221–1232 (2017).
29. Y. Fu, J. L. Huebner, V. B. Kraus, T. M. Griffin, Effect of aging on adipose tissue inflammation in the knee joints of F344BN rats. *J. Gerontol. A Biol. Sci. Med. Sci.* **71**, 1131–1140 (2016).
30. W. Liu *et al*., Effective treatment of steatosis and steatohepatitis by fibroblast growth factor 1 in mouse models of nonalcoholic fatty liver disease. *Proc. Natl. Acad. Sci. U.S.A.* **113**, 2288–2293 (2016).
31. M. G. A. Broeren *et al*., Suppression of the inflammatory response by disease-inducible interleukin-10 gene therapy in a three-dimensional micromass model of the human synovial membrane. *Arthritis Res. Ther.* **18**, 186 (2016).
32. I. C. Helmark *et al*., Exercise increases interleukin-10 levels both intraarticularly and peri-synovially in patients with knee osteoarthritis: A randomized controlled trial. *Arthritis Res. Ther.* **12**, R126 (2010).
33. M. Nakata *et al*., IL-10 gene transfer upregulates arcuate POMC and ameliorates hyperphagia, obesity and diabetes by substituting for leptin. *Int. J. Obes.* **40**, 425–433 (2016).
34. H. Kondo *et al*., Interleukin 10 treatment ameliorates high-fat diet-induced inflammatory atrial remodeling and fibrillation. *Circ. Arrhythm. Electrophysiol.* **11**, e006040 (2018).
35. S. Lacraz, L. P. Nicod, R. Chicheportiche, H. G. Welgus, J. M. Dayer, IL-10 inhibits metalloproteinase and stimulates TIMP-1 production in human mononuclear phagocytes. *J. Clin. Invest.* **96**, 2304–2310 (1995).
36. M. Kapoor, J. Martel-Pelletier, D. Lajeunesse, J. P. Pelletier, H. Fahmi, Role of proinflammatory cytokines in the pathophysiology of osteoarthritis. *Nat. Rev. Rheumatol.* **7**, 33–42 (2011).
37. L. A. Zúñiga *et al*., IL-17 regulates adipogenesis, glucose homeostasis, and obesity. *J. Immunol.* **185**, 6947–6959 (2010).
38. L. Chung *et al*., Interleukin 17 and senescent cells regulate the foreign body response to synthetic material implants in mice and humans. *Sci. Transl. Med.* **12**, eaax3799 (2020).
39. S. J. B. Snelling *et al*., Presence of IL-17 in synovial fluid identifies a potential inflammatory osteoarthritic phenotype. *PLoS One* **12**, e0175109 (2017).
40. F. Paré *et al*., *In vivo* protective effect of adipsin-deficiency on spontaneous knee osteoarthritis in aging mice. *Aging (Albany NY)* **12**, 2880–2896 (2020).
41. A. Larrañaga-Vera *et al*., Increased synovial lipodystrophy induced by high fat diet aggravates synovitis in experimental osteoarthritis. *Arthritis Res. Ther.* **19**, 264 (2017).
42. M. C. Lee *et al*., CCL17 blockade as a therapy for osteoarthritis pain and disease. *Arthritis Res. Ther.* **20**, 62 (2018).
43. M. F. Rai, T. Graeve, S. Twardziok, M. F. Schmidt, Evidence for regulated interleukin-4 expression in chondrocyte-scaffolds under in vitro inflammatory conditions. *PLoS One* **6**, e25749 (2011).
44. G. Wirnsberger, D. Hebenstreit, G. Posselt, J. Horejs-Hoeck, A. Duschl, IL-4 induces expression of TARC/CCL17 via two STAT6 binding sites. *Eur. J. Immunol.* **36**, 1882–1891 (2006).
45. Z. P. Fricker *et al*., Liver fat is associated with markers of inflammation and oxidative stress in analysis of data from the framingham heart study. *Clin. Gastroenterol Hepatol.* **17**, 1157.e4–1164.e4 (2019).
46. S. L. Kolasinski *et al*., 2019 American college of rheumatology/arthritis foundation guideline for the management of osteoarthritis of the hand, hip, and knee. *Arthritis Rheumatol.* **72**, 220–233 (2020).
47. D. K. White *et al*., Daily walking and the risk of incident functional limitation in knee osteoarthritis: An observational study. *Arthritis Care Res. (Hoboken)* **66**, 1328–1336 (2014).
48. T. M. Griffin, J. L. Huebner, V. B. Kraus, Z. Yan, F. Guilak, Induction of osteoarthritis and metabolic inflammation by a very high-fat diet in mice: Effects of short-term exercise. *Arthritis Rheum.* **64**, 443–453 (2012).
49. S. S. Glasson, T. J. Blanchet, E. A. Morris, The surgical destabilization of the medial meniscus (DMM) model of osteoarthritis in the 129/SvEv mouse. *Osteoarthritis Cartilage* **15**, 1061–1069 (2007).
50. A. I. Mina *et al*., CalR: A web-based analysis tool for indirect calorimetry experiments. *Cell Metab.* **28**, 656–666.e1 (2018).